Water Science & Technology

Water Science & Technology Vol 89 No 8, 1981 doi: 10.2166/wst.2024.112

Microplastic inhibits the sorption of trichloroethylene on modified biochar

Hainan Lu

State Environment Protection Engineering Center for Urban Soil Contamination Control and Remediation, Shanghai Academy of Environmental Sciences, Shanghai 200233, China
E-mail: luhn@saes.sh.cn

HL, 0009-0009-0618-510X

ABSTRACT

Biochar (BC) was used to remove trichloroethylene (TCE) from soil and water phases, and BC modification changed the sorption behavior of pollutants. Microplastics are emerging pollutants in the soil and water phases. Whether microplastics can affect the sorption of TCE by modified BC is not clear. Thus, batch sorption kinetics and isotherm experiments were conducted to elucidate the sorption of TCE on BC, and BC combined with polyethylene (PE) or polystyrene (PS). The results showed that HCl and NaOH modification increased TCE sorption on BC, while HNO_3 modification inhibited TCE sorption on BC. When PE/PS and BC coexisted, the TCE sorption capacity decreased significantly on BC-CK + PE, BC-HCl + PE, BC-HNO_3 + PE, BC-NaOH + PE, and BC-NaOH + PS, which was likely due to the preferential sorption of PE/PS on BC samples. We concluded that microplastics can change TCE sorption behavior and inhibit TCE sorption on BC samples. Thus, the interaction of BC and microplastics should be considered when BC is used for TCE removal in soil and water remediation.

Key words: biochar, microplastics, modification, sorption, trichloroethylene (TCE)

HIGHLIGHTS

- HCl and NaOH modification increased trichloroethylene (TCE) sorption on biochar.
- HNO_3 modification inhibited TCE sorption on biochar.
- Microplastics could change TCE sorption behavior.
- Polyethylene/polystyrene could preferentially adsorb onto biochar and inhibit TCE sorption by biochar samples.

GRAPHICAL ABSTRACT

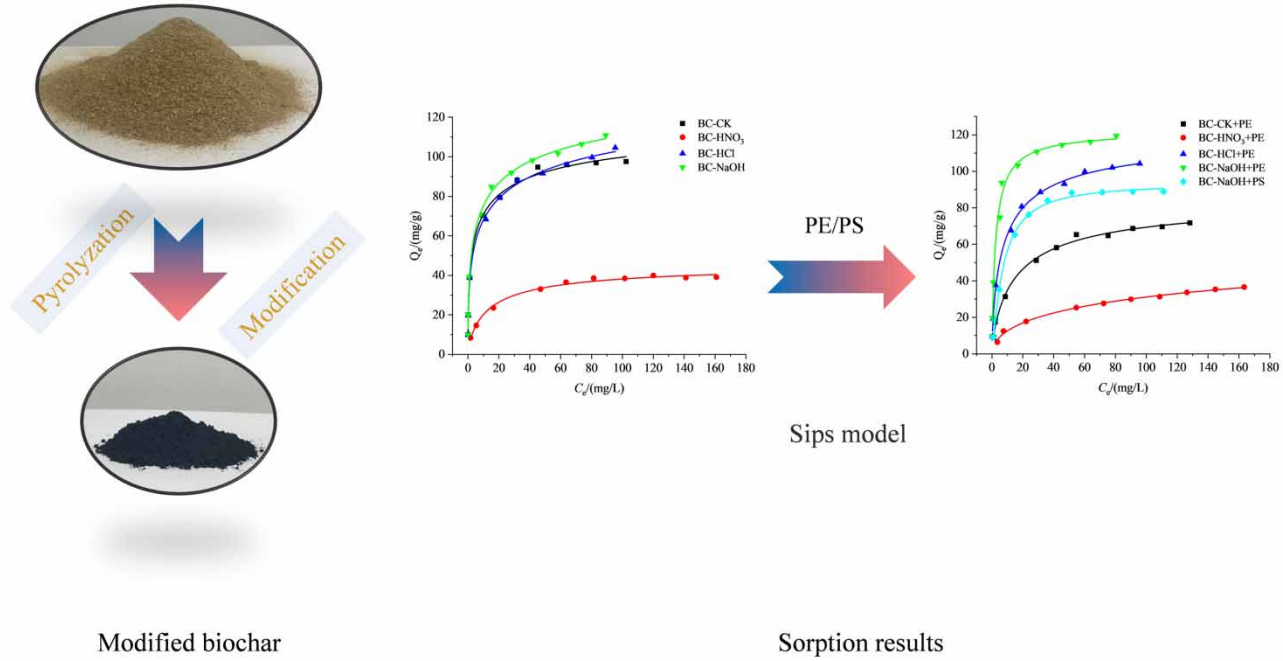

1. INTRODUCTION

Trichloroethylene (TCE) is one of the most common chlorinated solvents used in chemical, pharmaceutical, pesticide, and other industries (Siggins *et al.* 2020). TCE enters water, soil, and groundwater environments due to improper disposal processes, such as leakage and direct discharge, and pollutes these environments; as a result, it is a widespread pollutant in groundwater and soil environments. In some contaminated industrial sites, the concentration of TCE was found to reach hundreds of mg/L (Siggins *et al.* 2021). Due to the carcinogenic, teratogenic, and mutagenic effects of TCE, humans might develop cancer via long-term exposure to TCE-polluted environments. Thus, TCE has been categorized as a priority pollutant by agencies in many countries, such as the Ministry of Ecology and Environment of China, the United States Environmental Protection Agency (USEPA), and the European Commission (Ahmad *et al.* 2013).

Biochar (BC) is an excellent adsorbent for organic pollutants, which plays an important role in the removal of pollutants (Cao & Harris 2010). The large potential capacity of BC for pollutant adsorption can be ascribed to its unique properties, which include abundant functional groups, high specific surface area, and high aromaticity (Bao-Son *et al.* 2017). Moreover, modification can affect BC's properties and sorption capacities, improving pollutants' sorption. After HNO_3 modification, the methylene blue adsorption capacity of BC increased to 77.4 compared to 37.2 mg/g with unmodified BC (Wang *et al.* 2018). After NaOH modification, BC had a higher adsorption capacity for chloramphenicol (~2.1 mg/g) relative to BC without pretreatment (Fan *et al.* 2010). However, no studies have reported whether modification can affect TCE sorption on BC.

Multiple contaminants have been found in soil and water environments, and microplastics are among them. Recently, microplastics have emerged as concerned contaminants and are considered one of the most serious environmental pollutants. Residual plastic particles can be fragmented and gradually decomposed to form microplastics. In addition, some microplastics can be released from manufactured products. Microplastics have been detected in some lakes and rivers in many European countries, and their abundance can exceed 4×10^5 particles/km^2. Surface water environments in China also show microplastic pollution, and the abundance of microplastics floating in Taihu Lake reached 1.0×10^4 to 6.8×10^6 particles/km^2. In addition, 3.4×10^6 to 1.36×10^7 particles/km^2 of microplastics were found in the Three Gorges Reservoir area (Zhang *et al.* 2015; Su *et al.* 2016). Because of their high specific surface area and abundance of functional groups, microplastics can serve as potential carriers of organic contaminants (Dong *et al.* 2020). Therefore, understanding the environmental behavior of microplastics results in a better understanding of their interactions with organic pollutants.

Microplastics can adsorb organic pollutants via hydrophobic interactions, hydrogen bonding, halogen bonding, and π–π interactions (Bakir *et al.* 2012; Song *et al.* 2019; Wu *et al.* 2019; Mei *et al.* 2020). Microplastics were found to have strong adsorption capacities for polycyclic aromatic hydrocarbons and polychlorinated biphenyls. Organic pollutants can partition into the rubbery states of soft microplastics (such as polyethylene (PE) and polypropylene, etc.), and rigid microplastics (such as polystyrene (PS)) can adsorb organic pollutants via π–π interactions at their surfaces (Rochman *et al.* 2013; Zhang & Sun 2018). As a result, microplastics can adsorb and transfer organic pollutants, disrupting existing adsorption equilibria, which can change the bioavailability of organic pollutants.

Since microplastics are known to adsorb organic pollutants, it is expected that they can adsorb TCE; therefore, the sorption-based removal of TCE by BC would be affected by the coexistence of microplastics. However, no reports showing the effect of microplastics on the sorption behavior of TCE on BC have emerged. Furthermore, it has been reported that BC can interact with microplastics, which could influence the ability of BC to adsorb pollutants (Li *et al.* 2021). Moreover, the efficiency of TCE sorption can be affected by the interaction between BC and microplastics because of the abundant functional groups present on BC and microplastics.

To improve the understanding of potential interactions between BC and microplastics and the influence of these interactions on TCE sorption, sorption experiments were conducted to explore the TCE sorption behavior of BCs with different modifications and in the presence of microplastics (PE or PS). We hypothesize that (1) the two types of microplastics could inhibit the TCE sorption by BC and (2) these microplastics influence the sorption of TCE via interactions between BC and microplastics; the coexistence of microplastics affects the properties of the adsorbents. This study aimed to investigate the TCE sorption behavior of different modified BCs in the presence of microplastics. This research provides insights into the environmental behavior of TCE and microplastics. In addition, this study can serve as a guide for the application of BC to treat TCE-contaminated soil and water in which TCE and microplastics coexist.

2. MATERIALS AND METHODS

2.1. BC production, modification, and microplastics

Wheat straw was chosen for BC production. The production and modification of BC were performed as described in our previous studies (Lu *et al.* 2022). Briefly, the feedstocks were oven-dried and were ground and passed through a 0.355-mm sieve and then pyrolyzed at 700 °C in a muffle furnace under oxygen-limited conditions. The heating rate was 10 °C/min, and pyrolysis lasted for 2 h after the pyrolysis temperature was reached. Then, the obtained BC was passed through a 0.355-mm sieve again.

Three kinds of modifiers were used to treat the original BC: HCl, NaOH, and HNO_3 as common chemical modification (acidic, basic, and oxidized modification). The modification treatment process was as follows: original BC was added to 2 M of a modifier in a large glass beaker, and the solid-to-water ratio was 1:20 (weight/volume). Then, the beakers were placed on a magnetic stirrer for 4 h at 500 r/min and were then left undisturbed for 24 h. The treatment process was repeated to ensure complete modification. Subsequently, these BC samples were washed thoroughly with deionized water, oven-dried, and passed through a 0.355-mm sieve. These BC samples were labeled BC-M, in which M was the modifying agent. Two types of spherical microplastics were chosen for the experiment: PE (100 μm) and PS (100 μm), purchased from KXD Polymer Materials Co., Ltd. PE and PS were the most commonly used microplastics in daily life and in scientific research (Yang *et al.* 2021), which were the main plastic polymer types in sediment and water samples, e.g., sandy beaches (Zhou *et al.* 2021). In the realistic conditions, microplastics had different shapes such as fragments, particles, fibers/threads, and foams (Cordova *et al.* 2019). To circumvent or avoid as much as possible errors in adsorption effects caused by shape differences, beads were chosen for this study (Meng *et al.* 2024).

2.2. Materials characterization

The surface morphology of the BCs and microplastics was observed using scanning electron microscopy (SEM). Functional groups present on the BC samples and microplastics were analyzed using Fourier transform infrared (FTIR) spectroscopy in the range of 400–4,000 cm^{-1}. The elemental composition of the BC samples was analyzed by an elemental analyzer. The specific surface area parameters of the BC samples were analyzed by a Brunauer–Emmett–Teller (BET) analyzer. The aromatization characteristics of BC were characterized and analyzed by a DXR3xi Raman spectrometer (Thermo Scientific, USA). An excitation laser with a 532 nm wavelength was used in the test, and the recording spectrum ranged from 800 to 1,800 cm^{-1}.

2.3. Sorption kinetics experiments

Sorption kinetics experiments were conducted for TCE on all the BCs with/without microplastics at 25 °C. The BC samples and two kinds of microplastics were added individually or in combination to study the sorption behavior of TCE by BC-CK, BC-HCl, BC-NaOH, and BC-HNO_3; combinations of different modified BC sample and microplastic (BC-CK + PE, BC-HCl + PE, BC-NaOH + PE, BC-HNO_3 + PE); and combination of different microplastic (BC-NaOH + PS). The solid–aqueous ratio in the sorption experiment was 1:1,000 (w:v). An amount of 0.02 g of BC or 0.02 g of BC + 0.01 g of microplastic (for BC and microplastic combined treatment) mixed with 20 mL of solutions was added to 22-mL glass vials equipped with Teflon-lined screw caps. Na_2SO_4 (0.01 M) was added as the background solution. The amount and ratio of BC and microplastics used in this study were determined according to previous studies (Yao *et al.* 2023; Meng *et al.* 2024), in which the amount of BC and microplastics used in the reaction system was proven to be environmentally relevant and experimentally feasible. The initial concentration of TCE in aqueous solution was 100 mg/L. The glass vials were shaken in an oscillator at an agitation speed of 200 r/min. These samples were analyzed after 5, 10, 15, 30, and 60 min, and 3, 6, 12, 24, 48, and 72 h of shaking. Then, all samples were immediately filtered through a 0.22-μm filter for further analysis. Each treatment was carried out in triplicate.

2.4. Sorption isotherm experiments

Sorption isotherm experiments were conducted for TCE on all the BCs with/without microplastics in the dark at 25 °C. A series of TCE solutions ranging from 10 to 200 mg/L in concentration was prepared and then buffered with 0.01 M Na_2SO_4 to simulate natural water for batch-type adsorption experiments. With 20 mg of BC or 20 mg of BC + 10 mg of microplastic transferred to 22-mL glass vials equipped with Teflon-lined screw caps, 20 mL of solutions with TCE were mixed. These vials were sorption equilibrium in an oscillator at an agitation speed of 200 r/min for 24 h. Random standard and no-BC control samples were processed, and all samples were processed in triplicate. After the experiment, the supernatants of the samples were filtered through 0.22-μm nylon membranes.

2.5. Determination of TCE concentration

The TCE in solution was treated and then analyzed by gas chromatography equipped with an electron capture detector (GC-ECD, Agilent 7890B). Briefly, 1 mL of the experimental solution was removed and mixed with 1 mL of n-hexane, and the mixture was agitated at a speed of 200 r/min for 2 h and then vortexed for 2 min. Then, approximately 0.5 mL of the hexane phase with extracted TCE was transferred to a 1.8 mL vial for high-sensitivity TCE quantification using GC-ECD.

The GC-ECD instrument was equipped with an HP-5 capillary column (30 m × 320 μm × 0.25 μm, Agilent Technologies). The oven temperature was held at 40 °C for 5 min, ramped up to 50 °C at a rate of 8 °C min^{-1}, ramped up to 200 °C at a rate of 16 °C min^{-1}, and then held for 2 min. The inlet and detector temperatures were set to 200 and 320 °C, respectively. One microliter of liquid sample was injected into the GC at a split ratio of 20:1.

2.6. Quality control

To determine the recovery of TCE and TCE sorption to the glass vials during the sorption process, a treatment with the initial TCE concentration of 100 mg/L without adsorbent addition was used as a blank control in the sorption experiment. To determine the release of TCE from the original BC and microplastics during the sorption process, a treatment with 50 mg of adsorbent without TCE was used as a blank control, and no TCE was detected during the experiment.

2.7. Data analysis

The mass of TCE adsorbed per unit of adsorbent, q_e (mg/g), was calculated using the following equation:

$$q_e = \frac{(C_0 - C_e) \times V}{W} \tag{1}$$

where C_0 and C_e (mg/L) are the initial and equilibrium concentrations of TCE in aqueous phase, respectively, V (L) is the experimental volume of TCE in solution, and W (g) is the mass of the BC sample.

The experimental kinetics results were fitted with pseudo-first-order, pseudo-second-order, Elovich, and intraparticle diffusion models. The results of the isotherm experiments were fitted with the Freundlich, Langmuir, Sips, and Dubinin–Radushkevich (D–R) models. The specific equations and parameters used in the analyses are shown in the Supplementary

material (SI). The differences among the treatments were tested by independent *t* tests using SPSS 20.0 software. The significance for all statistical analyses was set to $\alpha = 0.05$.

3. RESULTS AND DISCUSSION

3.1. The properties of BC and microplastics

SEM images of the BC and microplastics (PE and PS) are shown in Figure 1. The PE and PS microplastics were spherical regular particles and had smooth surfaces, with a relatively uniform particle size (100 μm). The BC exhibited an uneven sheet-like structure, with a rough surface structure and disordered distribution. The pore structure of BC was rich, with wrinkles and cavities. The micromorphology of BC was affected by modification. The original BC's flakes and pores showed many attached substances, which occupied many adsorption sites of the BC. After modification, a large amount of the attachments on the BC surface were removed, resulting in a smoother surface and many exposed adsorption sites.

The functional groups on BC, PE, and PS played important roles in TCE sorption. The FTIR spectral characteristics of the BC and microplastic samples were analyzed in the range of 400–4,000 cm^{-1}, and several common functional groups were detected, as shown in Figure 2. Absorption peaks of –C–OH and –C–C– were observed in the BC samples, while the absorption peaks of –C = C–, –C = O, and $-CH_2$ disappeared in the BC samples. In previous studies, modifiers were shown to change functional group types. For example, an increase in the band at ~1,700 and at ~1,587 cm^{-1} was observed upon modification with HNO_3, HCl, and H_2SO_4, which was attributed to the formation of carbonyl structures and amide $-NH_2$ groups on BC (Boguta *et al.* 2019); H_2O_2 oxidation increased the quantity of carboxylic, lactone, and hydroxyl groups (Sajjadi *et al.* 2019); the number of acidic functional groups (e.g., carboxylic and phenolic groups) was reduced due to neutralization, while the amount of some acidic groups increased using NaOH modification (Li *et al.* 2017a). However, only a slight change was observed in the chemical bonds on the BC surface after modification (Lu *et al.* 2022). In the infrared spectrum of the PE sample, the antisymmetric stretching vibration of $-CH_2$ at 2,920 cm^{-1}, the symmetric stretching vibration of $-CH_2$ at 2,852 cm^{-1}, the in-plane angular vibration of $-CH_2$ at 1,469 cm^{-1}, and the in-plane swaying vibration of $-CH_2$ at 719 cm^{-1} were observed. As a polymer material, the PS samples had many sharp spectral bands. The infrared spectrum mainly consisted of two groups: the stretching vibration of the benzene ring (1,600, 1,580, 1,490, and 1,450 cm^{-1}) and the stretching vibration (3,100–3,000 cm^{-1}) of –CH on the benzene ring, as well as in-plane angular vibration (1,069, 1,028, and 540 cm^{-1}) and in-plane angular vibration (750 cm^{-1}) of –CH on the benzene ring (Kumar *et al.* 2021).

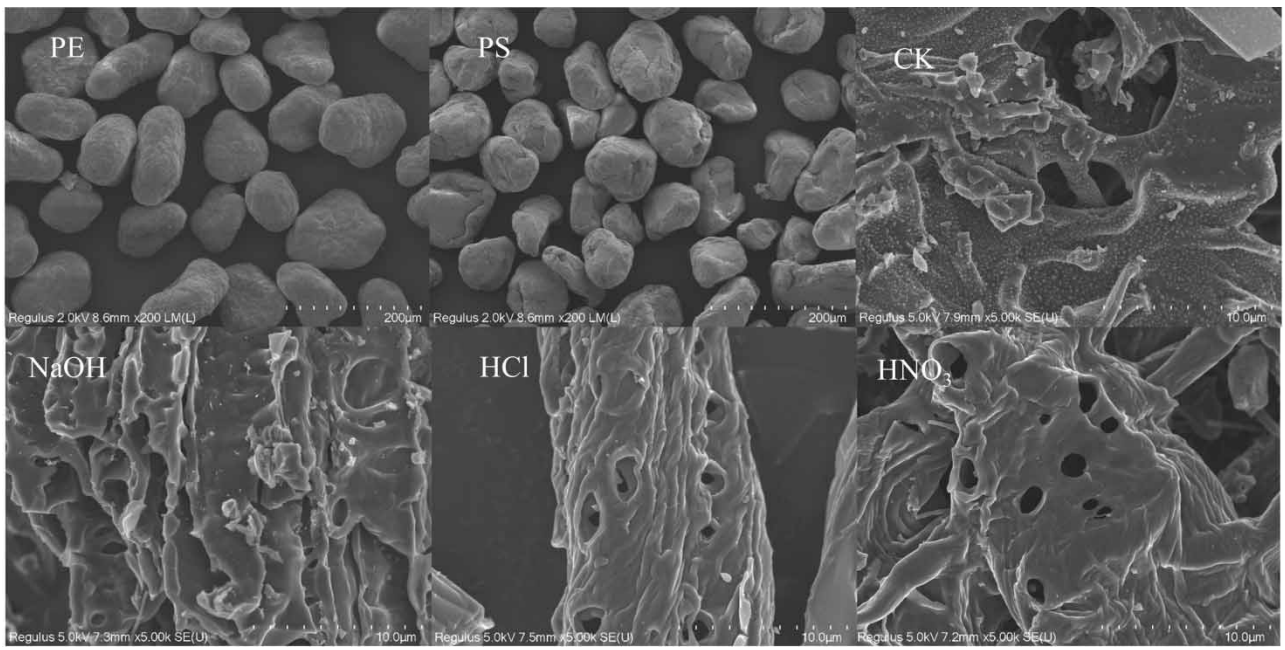

Figure 1 | SEM images of the BC samples, PE, and PS.

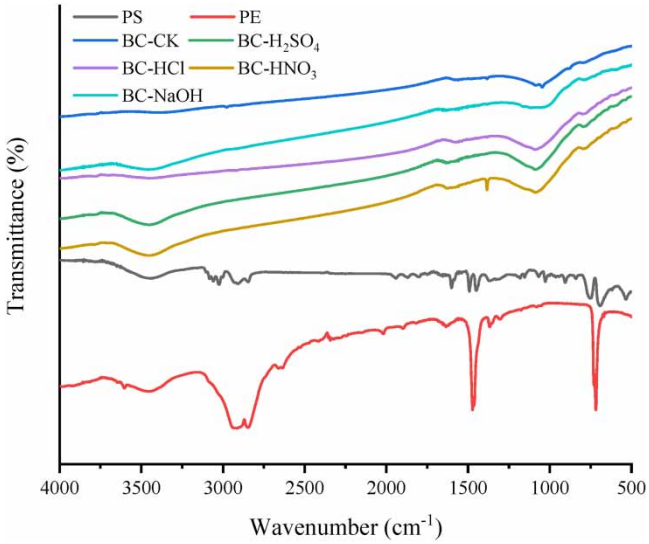

Figure 2 | FTIR spectra of the BC samples, PE, and PS.

The total, micropore, and mesopore surface areas measured through the BET, Horvath–Kawazoe and Barrett–Joyner–Halenda methods are shown in Table 1. For the initial BC samples, the total surface area was 202.3 m^2/g, the micropore surface area was 219.6 m^2/g, and the mesopore surface area was 71.6 m^2/g, which indicated a micropore-dominant structure. The total, micropore, and mesopore surface areas of the HCl-, NaOH-, and HNO_3-modified BC were 143.0–287.1, 171.1–350.6, and 111.0–123.0 m^2/g, respectively. The largest total and micropore surface areas were observed in the HCl-modified BC (287.1 and 350.6 m^2/g), and the lowest total and micropore surface areas were observed in the HNO_3-modified BC (143.0 and 171.1 m^2/g). The total, micropore, and mesopore surface areas of the PS sample were 0.594, 0.420, and 1.040 m^2/g, respectively, and the total, micropore, and mesopore surface areas of the PE sample were 0.292, 0.194, and 0.415 m^2/g, respectively. These results indicated that these microplastics were mainly solid with almost no voids.

The surface area of BC can be altered by modification to enhance BC sorption capacity for various pollutants. HCl solution can be used to increase the surface area of BC by removing precipitated salts and impurities from the pores of the carbonaceous sorbent and opening blocked pores in the pristine BC (Petrovic *et al.* 2016). Different acidic agents resulted in different modifications to BC. In this research, BC modified with hydrochloric acid was more effective for increasing surface area. Alkali modification is often used to improve the sorption ability of BC. Alkali modification can result in larger surface areas with additional surface hydroxyl groups, and BCs with higher surface areas have been reported after modification with KOH or NaOH (Guzel *et al.* 2017). Alkaline substance can result in the formation of new alkaline species, oxides, and carbonates via intercalation within a layer of BC crystallites. These species might penetrate the internal structure of the carbon matrix, widening existing pores and creating new pores (Pourret & Houben 2018). Because of its strong oxidizing capability,

Table 1 | Total, micropore, and mesopore surface areas of all the samples

	TSA (m^2/g)	MiSA (m^2/g)	MeSA (m^2/g)
PE	0.19	0.41	0.29
PS	0.42	1.04	0.59
BC-CK	219.6	71.66	202.3
BC-HNO_3	171.1	123.0	143.0
BC-HCl	321.5	111.0	264.7
BC-NaOH	350.6	120.2	287.1

TSA, total surface area; MiSA, micropore surface area; MeSA, mesopore surface area.

HNO_3 was commonly used as oxidizers to increase the amount of O-containing functional groups in BC. In some studies, HNO_3 modification decreased surface area by causing degradation of the micropore walls due to its erosive nature (Premarathna *et al.* 2019), and H_2O_2 modification decreased the surface area of BC. However, oxidation decreased the total and micropore surface areas of the samples in this study. HNO_3 might corrode the mesopores of BC, which could increase the total and micropore surface areas of BC. An enhancement in pore development via modification can increase the number of supporting sites for the sorption of pollutants.

The elemental composition, aromaticity index (AI), polarity index, and double-bond equivalents (DBEs) of the BC samples are listed in Table S1. The AI was used to characterize the degree of carbonization of BC samples and was calculated using the H/C ratio, and DBEs were used as an index to estimate the degree of unsaturation and were related to the density of C–C double bonds in BC (Pan & Guan 2010). The value of (O + N)/C was used to characterize the polarity of BC. The decreased AI and polarity index and increased DBE indicated increased carbonization and aromaticity of BC. For the BC samples, NaOH and HCl modification decreased the AI, but HNO_3 modification increased the AI. The DBE of all modified BC samples slightly decreased.

3.2. TCE sorption kinetics

Sorption kinetics was used to characterize the sorption process and clarify related sorption mechanisms. The sorption kinetics of TCE on BC and BC + PE/PS are presented in Figure 3. TCE was rapidly adsorbed by BC samples within 2 h and then absorbed slowly until adsorption equilibrium was reached (within 12 h). For this experiment, the equilibrium adsorption capacities of BC-CK, BC-HNO_3, BC-HCl, and BC-NaOH were 78.48, 38.85, 80.18, and 87.18 mg/g, respectively.

The sorption process could be well fitted by pseudo-second-order models (0.998–1) (Table S2), suggesting that both chemical and physical sorption mechanisms were involved in the BC and BC + PE/PS sorption processes. The calculated sorption amount based on the pseudo-second-order models approached the actual sorption amount from the batch sorption experiments, further indicating that TCE sorption was in line with the pseudo-second-order models. These results suggested that physical diffusion was not the main adsorption process, chemical adsorption might be the main adsorption process, and the rate-limiting step of the sorption process might be related to TCE chemisorption onto active sorption sites on the BC/microplastics surface. From the perspective of rate constants (*k*s), *k*s was in the order of BC-HNO_3 > BC-CK > BC-NaOH > BC-HCl.

After microplastic addition, the *k*s of BC-HNO_3 + PE decreased significantly, while the *k*s of BC-CK + PE increased; moreover, the *k*s of BC-NaOH + PE and BC-HCl + PE had no significant changes. The Elovich model describes a chemical sorption process that occurs on a heterogeneous surface (Diagboya *et al.* 2015). The Elovich model did not fit the sorption kinetics better than the pseudo-second-order model, indicating that physical sorption affected TCE sorption onto BC and BC + PE/PS. In the Elovich model, the chemical bonding strength of TCE with BC-HNO_3 was weaker than that of the other BC samples according to the desorption constant (β) (Table S2). HCl and NaOH modification enhanced the chemical bonding strength of TCE by BC. After microplastic addition, the chemical bonding strength of TCE was generally enhanced, further confirming that chemisorption was involved in TCE sorption. Moreover, the peaks for the functional groups did not significantly change after TCE sorption, which also indicated that physical processes were involved in the sorption mechanism.

The intraparticle diffusion model was chosen to explore the mass transfer steps and the critical stages controlling the TCE sorption process. According to the intraparticle diffusion model (Table S3), TCE sorption includes liquid film diffusion, surface sorption, and particle internal diffusion (Jia *et al.* 2013). The fitting results of the intraparticle diffusion model indicated a three-stage sorption process in TCE sorption regardless of the type of adsorbent studied (Figure 1). This is a common sorption mechanism for TCE (Ahmad *et al.* 2013). The first stage was a fast sorption process involving film diffusion of TCE from aqueous onto the surface of adsorbents. In this process, the sorption rates ($k_{3\text{-}1}$) were BC-HCl > BC-NaOH > BC-CK > BC-HNO_3, and similar trends in $k_{3\text{-}1}$ were observed when microplastics and BCs coexisted. However, the k_1 of BC-HCl + PE and BC-NaOH + PE was higher than that of BC-HCl and BC-NaOH, and the k_1 of BC-CK + PE and BC-HNO_3 + PE was lower than that of BC-CK and BC-HNO_3, which indicated that different effects were observed on the sorption of TCE by modified BC after PE addition. The second stage describes a relatively slow sorption process associated with surface sorption. In this process, the sorption rates ($k_{3\text{-}2}$) of TCE decreased in the order BC-HCl > BC-NaOH > BC-CK > BC-HNO_3, which was similar to k_1. However, the $k_{3\text{-}2}$ of the mixture of microplastics and BC increased. The third stage describes a slow sorption process associated with particle internal diffusion, and the fitted lines for this stage did not pass through the origin,

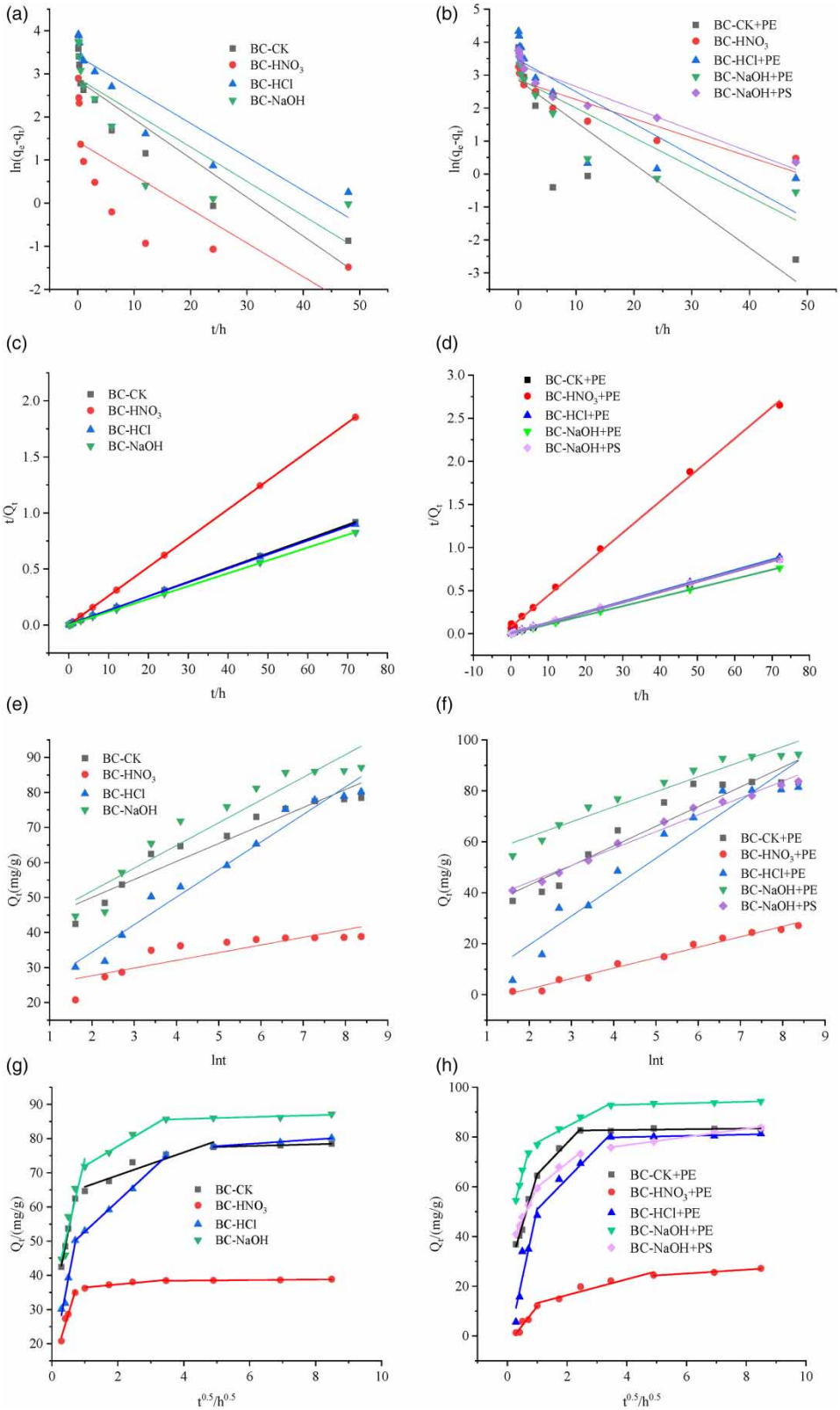

Figure 3 | Sorption kinetics of TCE onto adsorbents. Sorption kinetics of TCE on BC as fitted by (a) pseudo-first-order, (c) pseudo-second-order, (e) Elovich, and (g) intraparticle diffusion models, and on the mixed adsorbents of BC + PE/PS as fitted by (b) pseudo-first-order, (d) pseudo-second-order, (f) Elovich, and (h) intraparticle diffusion models.

indicating that particle internal diffusion is not the rate-limiting step during TCE sorption (Mirmohamadsadeghi *et al.* 2012). The mixing of microplastics with BC increased the sorption rate in the fast sorption stage ($k_{3\text{-}1}$), resulting in an increase in TCE sorption on BC + PE compared with BC alone. However, the k_1 of BC-HNO_3 was significantly lower after PE addition, indicating that PE inhibited TCE sorption by BC-HNO_3.

3.3. TCE sorption isotherm

The sorption isotherms of TCE by BC samples and mixed BC and microplastics are shown in Figure 4. Freundlich, Langmuir, Sips, and D–R models were used to describe the sorption behavior, and the fitting parameters are listed in Tables S4 and S5. The Langmuir model assumes that all active sites have the same energy and that adsorption occurs in monolayers without interaction (Nguyen *et al.* 2021). The Freundlich model presumes that the activation energy is nonequal and multilayer adsorption occurs (Zhang *et al.* 2018), and the Sips model is a combination of the Freundlich and Langmuir models (Zhou *et al.* 2018). The D–R model is commonly used to describe the adsorption process and mechanism of porous materials (Ngwabebhoh *et al.* 2016).

The isotherms of TCE displayed a nonlinear trend with a concave-downward curvature at low concentrations of TCE and a linear shape at high concentrations of TCE. Within the concentration range (0–200 mg/L) of TCE in this experiment, a negative effect of the sorption of TCE by BC-HNO_3 was observed. Enhanced sorption of TCE by BC-HCl and BC-NaOH was observed. These results demonstrated that the effect of modification on BC sorption performance varied.

According to Table S4, the sorption isotherms of TCE by BC-HNO_3 were better fitted by the Langmuir model than by the Freundlich model, and the sorption isotherms of TCE by BC-CK, BC-HCl, and BC-NaOH were better fitted by the Freundlich model than by the Langmuir model. These results demonstrated that TCE sorption onto BC-HNO_3 was a single-layer sorption process, while TCE sorption onto BC-CK, BC-HCl, and BC-NaOH was a multilayer sorption process. This study revealed for the first time that the adsorption of TCE exhibits different sorption processes on different BC with/without microplastics. After microplastics were added, the model fitting results changed. The sorption isotherms of TCE by BC-HNO_3 + PE were better fitted by the Freundlich model than by the Langmuir model, while the sorption isotherms of TCE by BC-CK + PE, BC-HCl + PE, and BC-NaOH + PE were better fitted by the Langmuir model than by the Freundlich model. These results demonstrated that PE changed the TCE sorption behavior of BC. PS had the same trend for TCE sorption because BC-NaOH + PS was fitted better by the Langmuir model than by the Freundlich model; however, the sorption of TCE by BC-NaOH + PS was lower than that by BC-NaOH + PE. The nonlinear constants ($1/n$) were far lower than 1 ($1/n$ was in the range of 0.31–0.63), suggesting that nonlinear surface adsorption was important in the TCE sorption process (Table S4). Moreover, according to the $1/n$ ranges, TCE sorption onto BC samples fell in a favorable zone ($0.1 < 1/n < 0.5$), while that onto BC + PE/PS fell in a pseudolinear zone ($0.5 < 1/n < 1.0$)(Tseng & Wu 2008), indicating that the surface adsorption of TCE was enhanced upon the mixing of microplastics and BCs. According to the Langmuir model, the sorption capacity (Q_m) was the highest on BC-NaOH (101.62 mg/g), followed by BC-CK (95.33 mg/g) and BC-HCl (94.75 mg/g), and was the lowest on BC-HNO_3 (42.28 mg/g) when PE was absent. When PE was added, the highest Q_m of TCE was observed on BC-NaOH + PE (119.93 mg/g), followed by BC-HCl + PE (106.00 mg/g) and BC-CK + PE (76.68 mg/g), and the lowest Q_m was observed on BC-HNO_3 (39.75 mg/g). These results demonstrated that PE inhibited the sorption of TCE by BC-CK, slightly inhibited the sorption of TCE by BC-HNO_3, and increased the sorption of TCE by BC-NaOH and BC-HCl. The effect of PS on the adsorption of TCE by BC-NaOH was different from that of PE, and the Q_m of BC-NaOH + PS was 99.25.

For the D–R model, the sorption isotherms of TCE by all samples showed the poorest fits, indicating that the D–R model was not suitable for the sorption isotherms. The sorption energy (E_α) of the D–R model was 0.342–3.959 kJ/mol lower than 8 kJ/mol. For the Sips model, the sorption isotherms of TCE by BC and BC + microplastics fit better than the Langmuir and Freundlich models, demonstrating that monolayer and multilayer adsorption were involved in the sorption behavior of TCE in all samples. According to the Q_m of the Sips model, the highest sorption capacity for TCE was observed on BC-NaOH, at 154.13 mg/g, followed by BC-HCl and BC-CK, and the lowest Q_m was 46.56 mg/g on BC-HNO_3, indicating that HCl and NaOH modification enhanced the sorption of TCE, while HNO_3 modification inhibited the sorption of TCE when PE was absent. When PE was added, the Q_m of BC-NaOH + PE and BC-HCl + PE had similar sorption capacities for TCE (122.33 and 122.30 mg/g, respectively), followed by BC-CK + PE (86.34 mg/g). The lowest sorption capacity of TCE was 44.36 mg/g on BC-HNO_3 + PE. The most significant inhibitory effect was observed on BC-CK + PE. For PS microplastics, the Q_m of BC-NaOH + PS was 93.79 mg/g, which was lower than that of BC-NaOH (150.71 mg/g) and BC-NaOH + PE (122.33 mg/g), indicating that PS significantly inhibited the sorption of TCE by BC-NaOH compared with PE microplastics.

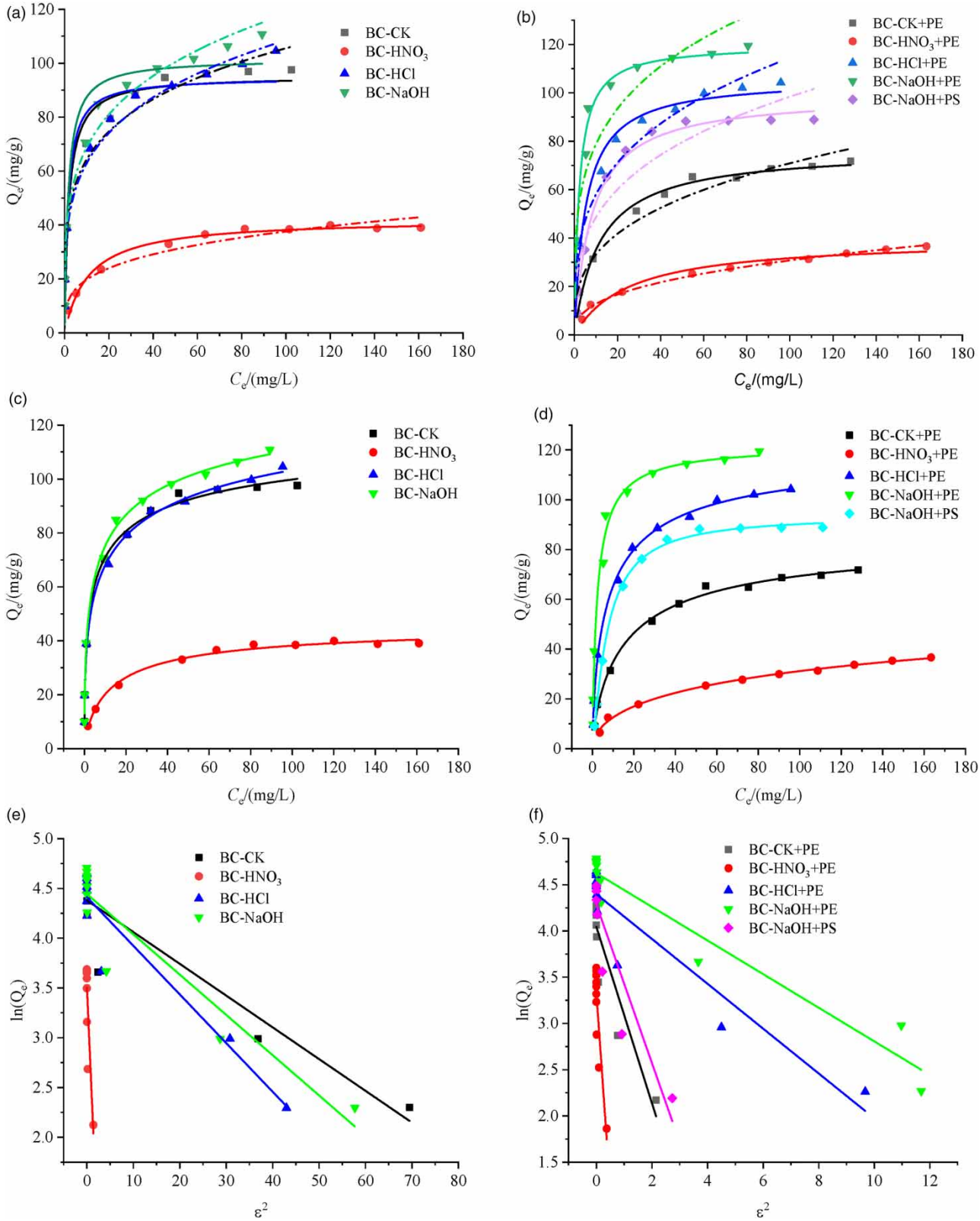

Figure 4 | Sorption isotherms of TCE onto adsorbents. Sorption isotherms of TCE on BC as fitted by the (a) Langmuir (solid curves) and Freundlich (dashed–dotted curves), (c) Sips, and (e) D–R models. Sorption isotherms of TCE on BC + PE/PS as fitted by (b) Langmuir (solid curves) and Freundlich (dashed–dotted curves), (d) Sips, and (f) D–R models.

3.4. Impact of the sorption behavior on TCE

BC showed stronger sorption of TCE relative to the microplastics because of BC's high specific surface area and microporosity, predominantly absorbing via pore filling (Schreiter *et al.* 2018). In addition, BC produced at higher temperatures showed greater TCE sorption capacity from water due to its high surface area, microporosity, and degree of carbonization (Ahmad *et al.* 2012, 2013). Among the Sips sorption isotherm models, the fit was better than that of the Freundlich and Langmuir models, indicating that both single- and multilayer sorption processes occurred. HNO_3 modification inhibited TCE sorption, and NaOH and HCl modification enhanced TCE sorption. According to characterization data from a previous study (Lu *et al.* 2022), HNO_3 modification reduces the aromaticity, total specific surface area, and micropores in BC while increasing the polarity of BC. However, HCl and NaOH modification improved the aromaticity, total specific surface area, and micropore area of BC while reducing the polarity of BC. HNO_3 modification inhibited TCE sorption on BC by reducing the pore filling and hydrophobic effects of BC, while the nitro functional group formed on the surface of BC after modification could inhibit the sorption of TCE. HCl and NaOH modification might promote TCE sorption on BC by improving the pore filling and hydrophobic effects of BC.

When BC was modified by acidic or basic agents, the properties of BC changed. Based on the Langmuir and Freundlich fitting parameters, the Langmuir fit for HNO_3-modified BC was better, and the Freundlich fits for CK, HCl-, and NaOH-modified BC were better. These results demonstrated that single-layer sorption was dominant on HNO_3-modified BC, while multilayer sorption was dominant on CK, HCl-, and NaOH-modified BC. HNO_3 modification affected the structure of BC, changing the sorption behavior of TCE. N–O bonds (nitro groups and nitrate complexes in BC) could increase after HNO_3 modification (Sajjadi *et al.* 2019), and some inorganic substances could be dissolved, including active components such as SiO_2, Al_2O_3, Fe_2O_3, K_2O, and Na_2O and some impurities such as CaO and MgO, which are able to react with HNO_3 (Sajjadi *et al.* 2019). Moreover, micropores would be narrowed or blocked by oxygen groups formed on the entrance and walls of pores, leading to a change in the pore structure of the BC. HCl solution was often used to remove precipitated salts and impurities from the pores of carbonaceous sorbents such as BC to increase specific surface area (Zhang *et al.* 2007). HCl treatment increases the quantity of weakly acidic oxygen-containing functional groups and single-bonded oxygen-containing functional groups such as phenols, ethers, and lactones (Chen & Wu 2004; Tong *et al.* 2016). NaOH is often used to activate carbon to generate pores via four phenomena: (i) creation of new pores, (ii) opening of previously inaccessible pores, (iii) widening of existing pores, and (iv) merging of existing pores due to pore wall breakage (Yang *et al.* 2010). By using NaOH, the number of acidic functional groups (e.g., carboxylic and phenolic groups) are reduced because of neutralization, while the amount of lactone groups might increase (Li *et al.* 2017a, 2017b, 2017c, 2017d). This might be the reason that HNO_3 modification inhibited TCE sorption, while HCl and NaOH modification promoted TCE sorption.

When PE or PS microplastic was added, the TCE sorption behavior of BC was altered. The fit for the Sips sorption isotherm model was better than that of the Freundlich and Langmuir models, which also indicated that both single- and multilayer sorption processes were involved in TCE sorption by BC + PE/PS. Compared with no microplastic addition, BC-CK + PE, BC-HCl + PE, BC-NaOH + PE, and BC-NaOH-PS significantly inhibited TCE sorption, and a slight inhibition of TCE sorption by BC-HNO_3 + PE was observed. This might be due to the sorption of BC on PE/PS, which consumed sorption sites on BC, resulting in the inhibition of TCE sorption.

Moreover, according to the Sips, Langmuir, and Freundlich sorption isotherms of the BC samples and BC + PE/PS samples, although both single- and multilayer adsorption occurred in these sorption processes, the dominant mechanism of sorption of HNO_3-modified BC transitioned from single- to multilayer sorption, while the dominant sorption mechanism of CK, HCl-, and NaOH-modified BC transitioned from multilayer to single-layer sorption when PE or PS was present. These results indicated that microplastics changed the TCE sorption behavior (Kumar *et al.* 2023).

The FTIR and Raman spectral characteristics of BC and BC + PE/PS were analyzed before and after the sorption process (Figures S1 and S5). There was a slight change in the FTIR spectrum after the sorption process. Raman spectroscopy can be used to quantify the structural defects and disorders in BC samples, mainly considering the two prominent first-order peaks denoted G ($-1{,}580\ cm^{-1}$) and D ($-1{,}350\ cm^{-1}$). The ratio of the D band to the G band (ID/IG) is typically utilized to investigate structural defects and the degree of graphitization of carbon materials (Smith *et al.* 2016; Zhong *et al.* 2021). As shown in Figure 5, the ID/IG value decreased after BC absorbed TCE, indicating that the aromatic ring structure in BC participated in the TCE sorption process when microplastics were absent. However, when PE/PS was added, the ID/IG value of the BC sample decreased more significantly, which might be due to the preferential sorption of PE/PS, causing a decrease in the

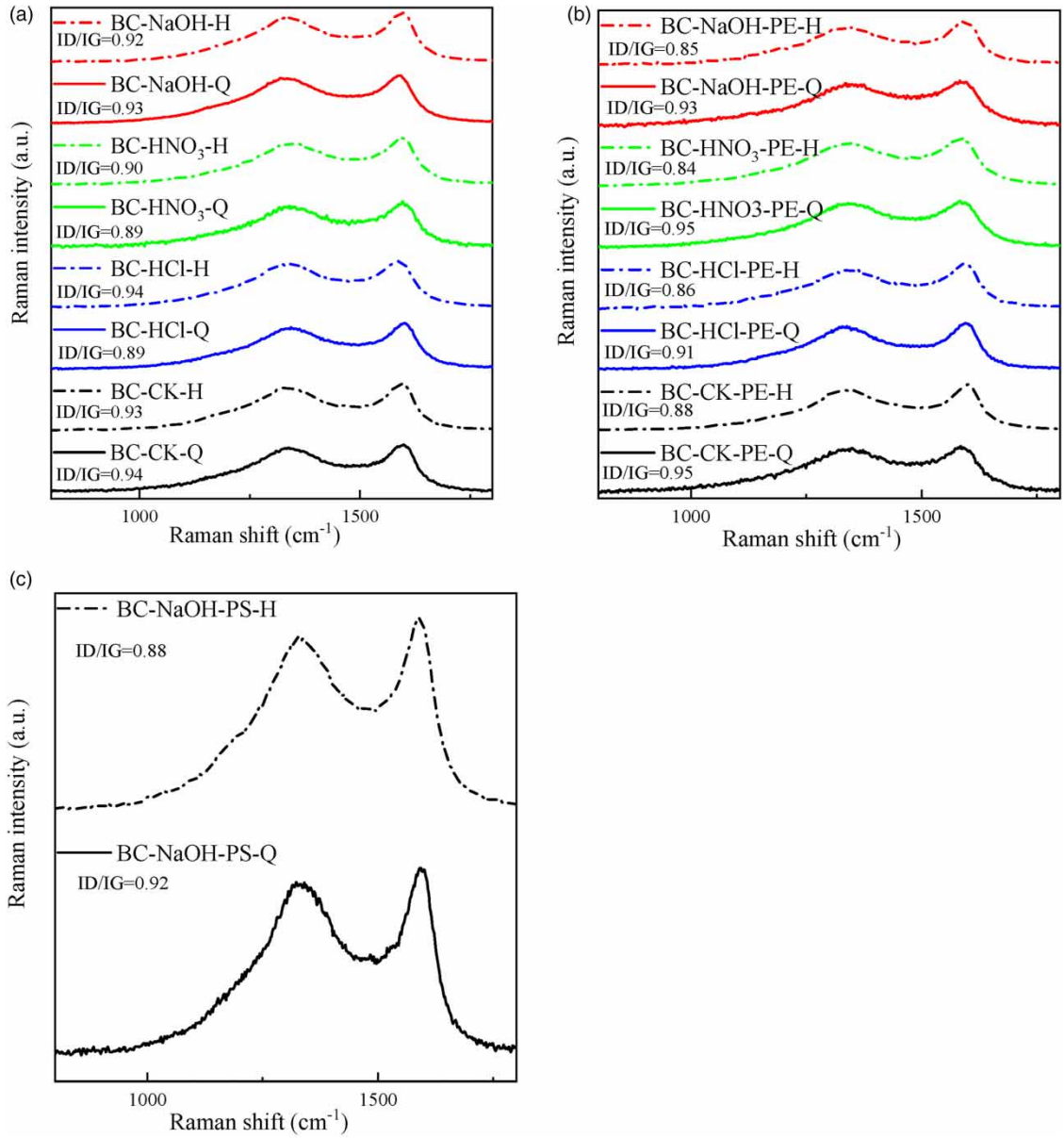

Figure 5 | Raman spectral characteristics of all samples before and after the sorption process. H, after the sorption process; Q, before the sorption process.

number of sorption sites on BC-NaOH + PS. Compared to BC-NaOH + PE, BC-NaOH-PS significantly inhibited TCE sorption, which might be due to interactions between the benzene ring structure of PS and BC-NaOH, which caused a decrease in the number of sorption sites on BC-NaOH.

Because of their hydrophobicity, microplastics can be attracted to adsorption sites on BC due to hydrophobic interactions in aqueous media (Fu *et al.* 2021; Wang *et al.* 2021). Furthermore, the adsorption of microplastics onto BC surfaces could occur via electrostatic attraction, physical attachment, or surface complexation due to the presence of carboxyl groups (Beckingham & Ghosh 2017; Ye *et al.* 2020; Li *et al.* 2021). In this sorption process, microeffects such as electrostatic interactions, hydrophobicity, specific surface area, pore filling, and H-bonding played roles in the adsorption of TCE by different BC samples. However, in this study, the microplastic particles used were larger (100 μm). The macroeffects might be another important reason for the sorption of TCE by the combinations of 100-μm microplastic particles and BC samples (Wang *et al.* 2020). First, the large size of the microplastic could block the pores on the surface of BC samples, which might make the

sorption behavior of TCE by BC inclined toward surface sorption. Second, BC contains many flaky shaped particles, and the microplastic particles were likely entangled with the BC via electrostatic interactions, which might cause pore filling to become the main adsorption behavior process (Yang *et al.* 2017; Wang *et al.* 2020). Moreover, considering the presence of other coexisting pollutants (e.g., organochlorine pesticides, organophosphorus pesticides, and antibiotics) in actual industrial wastewater, future research was needed to expand the range of pollutants studied to improve the general applicability of this research. Meanwhile, microplastics were a class of polymers with numerous chemical additives. For example, phthalate esters (PAEs) were one of the most commonly used microplastic additives. BC had been found to adsorb PAEs through pore filling, H-bonding, and p-p electron donor-acceptor (EDA) interactions (Ma *et al.* 2019; Ghosh & Sahu 2023), which might reduce the number of BC adsorption sites available for other organic pollutants. Thus, in addition to direct adsorption, the interactions between microplastics and BC, which involve the release of endogenous additives of microplastics, should be given more attention in future studies because this process could further affect the removal of target pollutants by BC.

4. CONCLUSIONS

Modification changed the TCE sorption behavior of BC, and HNO_3 modification inhibited TCE sorption by reducing the aromaticity, total specific surface area, and micropores in BC and by increasing the polarity of BC. HCl and NaOH modification increased TCE sorption by increasing the aromaticity, total specific surface area, and micropore area of BC and reducing the polarity of BC. The interaction between BC and microplastics changed the properties of the TCE sorption process. PE and PS could be attracted to the adsorption sites on BC to inhibit TCE sorption; as a result, the sorption behavior shifted from multilayer to single-layer sorption on BC-CK, BC-HCl, and BC-NaOH, while it shifted from single- to multilayer sorption on BC-HNO_3. Thus, coexisting microplastics cannot be neglected during the evaluation of the TCE sorption behavior of BC. This study provides a new insight into the sorption behavior of BC under conditions where microplastics and TCE coexist. Furthermore, future studies should be conducted on the effects of actual industrial wastewater and endogenous additives of microplastics to improve the general applicability of the results.

ACKNOWLEDGEMENTS

The author would like to thank Jiacheng Xu and Peng Li for their technical and experimental assistance, and Jingke Sima for providing funding from the National Natural Science Foundation of China (No. 42107448).

DATA AVAILABILITY STATEMENT

All relevant data are included in the paper or its Supplementary Information.

CONFLICT OF INTEREST

The authors declare there is no conflict.

REFERENCES

Ahmad, M., Lee, S. S., Dou, X., Mohan, D., Sung, J.-K., Yang, J. E. & Ok, Y. S. 2012 Effects of pyrolysis temperature on soybean stover- and peanut shell-derived biochar properties and TCE adsorption in water. *Bioresource Technology* **118**, 536–544.

Ahmad, M., Lee, S. S., Rajapaksha, A. U., Vithanage, M., Zhang, M., Cho, J. S., Lee, S.-E. & Ok, Y. S. 2013 Trichloroethylene adsorption by pine needle biochars produced at various pyrolysis temperatures. *Bioresource Technology* **143**, 615–622.

Bakir, A., Rowland, S. J. & Thompson, R. C. 2012 Competitive sorption of persistent organic pollutants onto microplastics in the marine environment. *Marine Pollution Bulletin* **64** (12), 2782–2789.

Bao-Son, T., Werner, D. & Reid, B. J. 2017 Application of a full-scale wood gasification biochar as a soil improver to reduce organic pollutant leaching risks. *Journal of Chemical Technology and Biotechnology* **92** (8), 1928–1937.

Beckingham, B. & Ghosh, U. 2017 Differential bioavailability of polychlorinated biphenyls associated with environmental particles: Microplastic in comparison to wood, coal and biochar. *Environmental Pollution* **220**, 150–158.

Boguta, P., Sokolowska, Z., Skic, K. & Tomczyk, A. 2019 Chemically engineered biochar – Effect of concentration and type of modifier on sorption and structural properties of biochar from wood waste. *Fuel* **256**, 115893.

Cao, X. & Harris, W. 2010 Properties of dairy-manure-derived biochar pertinent to its potential use in remediation. *Bioresource Technology* **101** (14), 5222–5228.

Chen, J. P. & Wu, S. N. 2004 Acid/base-treated activated carbons: Characterization of functional groups and metal adsorptive properties. *Langmuir* **20** (6), 2233–2242.

Cordova, M. R., Purwiyanto, A. I. S. & Suteja, Y. 2019 Abundance and characteristics of microplastics in the northern coastal waters of Surabaya, Indonesia. *Marine Pollution Bulletin* **142**, 183–188.

Diagboya, P. N., Olu-Owolabi, B. I. & Adebowale, K. O. 2015 Synthesis of covalently bonded graphene oxide-iron magnetic nanoparticles and the kinetics of mercury removal. *RSC Advances* **5** (4), 2536–2542.

Dong, S., Xia, J., Wang, W., Liu, H. & Sheng, L. 2020 Review on impact factors and mechanisms of microplastic transport in soil and groundwater. *Transactions of the Chinese Society of Agricultural Engineering* **36** (14), 1–8.

Fan, Y., Wang, B., Yuan, S., Wu, X., Chen, J. & Wang, L. 2010 Adsorptive removal of chloramphenicol from wastewater by NaOH modified bamboo charcoal. *Bioresource Technology* **101** (19), 7661–7664.

Fu, L., Li, J., Wang, G., Luan, Y. & Dai, W. 2021 Adsorption behavior of organic pollutants on microplastics. *Ecotoxicology and Environmental Safety* **217**, 112207.

Ghosh, S. & Sahu, M. 2023 Adsorptive removal of dimethyl phthalate using peanut shell-derived biochar from aqueous solutions: Equilibrium, kinetics, and mechanistic studies. *Environmental Science and Pollution Research* **30** (37), 87599–87612.

Guzel, F., Saygili, H., Saygili, G. A., Koyuncu, F. & Yilmaz, C. 2017 Optimal oxidation with nitric acid of biochar derived from pyrolysis of weeds and its application in removal of hazardous dye methylene blue from aqueous solution. *Journal of Cleaner Production* **144**, 260–265.

Jia, M., Wang, F., Bian, Y., Jin, X., Song, Y., Kengara, F. O., Xu, R. & Jiang, X. 2013 Effects of pH and metal ions on oxytetracycline sorption to maize-straw-derived biochar. *Bioresource Technology* **136**, 87–93.

Kumar, B. N. V., Loeschel, L. A., Imhof, H. K., Loeder, M. G. J. & Laforsch, C. 2021 Analysis of microplastics of a broad size range in commercially important mussels by combining FTIR and Raman spectroscopy approaches. *Environmental Pollution* **269**, 116147.

Kumar, R., Verma, A., Rakib, M. R. J., Gupta, P. K., Sharma, P., Garg, A., Girard, P. & Aminabhavi, T. M. 2023 Adsorptive behavior of micro(nano)plastics through biochar: Co-existence, consequences, and challenges in contaminated ecosystems. *Science of the Total Environment* **856**, 159097.

Li, B., Yang, L., Wang, C.-Q., Zhang, Q.-P., Liu, Q.-C., Li, Y.-D. & Xiao, R. 2017a Adsorption of Cd(II) from aqueous solutions by rape straw biochar derived from different modification processes. *Chemosphere* **175**, 332–340.

Li, H., Mahyoub, S. A. A., Liao, W., Xia, S., Zhao, H., Guo, M. & Ma, P. 2017b Effect of pyrolysis temperature on characteristics and aromatic contaminants adsorption behavior of magnetic biochar derived from pyrolysis oil distillation residue. *Bioresource Technology* **223**, 20–26.

Li, H., Qiu, Y.-f., Wang, X.-l., Yang, J., Yu, Y.-j., Chen, Y.-q. & Liu, Y.-d. 2017c Biochar supported Ni/Fe bimetallic nanoparticles to remove 1,1,1-trichloroethane under various reaction conditions. *Chemosphere* **169**, 534–541.

Li, R., Wang, J. J., Zhou, B., Zhang, Z., Liu, S., Lei, S. & Xiao, R. 2017d Simultaneous capture removal of phosphate, ammonium and organic substances by MgO impregnated biochar and its potential use in swine wastewater treatment. *Journal of Cleaner Production* **147**, 96–107.

Li, X., Jiang, X., Song, Y. & Chang, S. X. 2021a Coexistence of polyethylene microplastics and biochar increases ammonium sorption in an aqueous solution. *Journal of Hazardous Materials* **405**, 124260.

Lu, H., Xu, J., Feng, Z., Li, F., Cao, X. & Yang, J. 2022 Effects of different modifiers on the sorption and structural properties of biochar derived from wheat stalk. *Environmental Science and Pollution Research* **29** (36), 54988–55002.

Ma, S. Q., Jing, F. Q., Sohi, S. P. & Chen, J. W. 2019 New insights into contrasting mechanisms for PAE adsorption on millimeter, micron- and nano-scale biochar. *Environmental Science and Pollution Research* **26** (18), 18636–18650.

Mei, W., Chen, G., Bao, J., Song, M., Li, Y. & Luo, C. 2020 Interactions between microplastics and organic compounds in aquatic environments: A mini review. *Science of the Total Environment* **736**, 139472.

Meng, Z. W., Wu, J. W., Huang, S., Xin, L. & Zhao, Q. 2024 Competitive adsorption behaviors and mechanisms of Cd, Ni, and Cu by biochar when coexisting with microplastics under single, binary, and ternary systems. *Science of the Total Environment* **913**, 169524.

Mirmohamadsadeghi, S., Kaghazchi, T., Soleimani, M. & Asasian, N. 2012 An efficient method for clay modification and its application for phenol removal from wastewater. *Applied Clay Science* **59–60**, 8–12.

Nguyen, L. H., Van, H. T., Chu, T. H. H., Nguyen, T. H. V., Nguyen, T. D., Hoang, L. P. & Hoang, V. H. 2021 Paper waste sludge-derived hydrochar modified by iron (III) chloride for enhancement of ammonium adsorption: An adsorption mechanism study. *Environmental Technology & Innovation* **21**, 101223.

Ngwabebhoh, F. A., Gazi, M. & Oladipo, A. A. 2016 Adsorptive removal of multi-azo dye from aqueous phase using a semi-IPN superabsorbent chitosan-starch hydrogel. *Chemical Engineering Research & Design* **112**, 274–288.

Pan, J. & Guan, B. 2010 Adsorption of nitrobenzene from aqueous solution on activated sludge modified by cetyltrimethylammonium bromide. *Journal of Hazardous Materials* **183** (1–3), 341–346.

Petrovic, J. T., Stojanovic, M. D., Milojkovic, J. V., Petrovic, M. S., Sostaric, T. D., Lausevic, M. D. & Mihajlovic, M. L. 2016 Alkali modified hydrochar of grape pomace as a perspective adsorbent of Pb^{2+} from aqueous solution. *Journal of Environmental Management* **182**, 292–300.

Pourret, O. & Houben, D. 2018 Characterization of metal binding sites onto biochar using rare earth elements as a fingerprint. *Heliyon* **4** (2), e00543.

Premarathna, K. S. D., Rajapaksha, A. U., Sarkar, B., Kwon, E. E., Bhatnagar, A., Ok, Y. S. & Vithanage, M. 2019 Biochar-based engineered composites for sorptive decontamination of water: A review. *Chemical Engineering Journal* **372**, 536–550.

Rochman, C. M., Hoh, E., Hentschel, B. T. & Kaye, S. 2013 Long-term field measurement of sorption of organic contaminants to five types of plastic pellets: Implications for plastic marine debris. *Environmental Science & Technology* **47** (3), 1646–1654.

Sajjadi, B., Zubatiuk, T., Leszczynska, D., Leszczynski, J. & Chen, W. Y. 2019 Chemical activation of biochar for energy and environmental applications: A comprehensive review. *Reviews in Chemical Engineering* **35** (7), 777–815.

Schreiter, I. J., Schmidt, W. & Schueth, C. 2018 Sorption mechanisms of chlorinated hydrocarbons on biochar produced from different feedstocks: Conclusions from single- and bi-solute experiments. *Chemosphere* **203**, 34–43.

Siggins, A., Abram, F. & Healy, M. G. 2020 Pyrolysed waste materials show potential for remediation of trichloroethylene-contaminated water. *Journal of Hazardous Materials* **390**, 121909.

Siggins, A., Thorn, C., Healy, M. G. & Abram, F. 2021 Simultaneous adsorption and biodegradation of trichloroethylene occurs in a biochar packed column treating contaminated landfill leachate. *Journal of Hazardous Materials* **403**, 123676.

Smith, M. W., Dallmeyer, I., Johnson, T. J., Brauer, C. S., McEwen, J.-S., Espinal, J. F. & Garcia-Perez, M. 2016 Structural analysis of char by Raman spectroscopy: Improving band assignments through computational calculations from first principles. *Carbon* **100**, 678–692.

Song, H., Luo, X., Zhang, L., He, B., Li, J. & Wang, Y. 2019 Characteristic analysis of methyl orange adsorption on microplastics in water. *Earth Science Frontiers* **26** (6), 19–27.

Su, L., Xue, Y., Li, L., Yang, D., Kolandhasamy, P., Li, D. & Shi, H. 2016 Microplastics in taihu lake, China. *Environmental Pollution* **216**, 711–719.

Tong, Y., Mayer, B. K. & McNamara, P. J. 2016 Triclosan adsorption using wastewater biosolids-derived biochar. *Environmental Science – Water Research & Technology* **2** (4), 761–768.

Tseng, R.-L. & Wu, F.-C. 2008 Inferring the favorable adsorption level and the concurrent multi-stage process with the Freundlich constant. *Journal of Hazardous Materials* **155** (1–2), 277–287.

Wang, Y., Zhang, Y., Li, S., Zhong, W. & Wei, W. 2018 Enhanced methylene blue adsorption onto activated reed-derived biochar by tannic acid. *Journal of Molecular Liquids* **268**, 658–666.

Wang, Z., Sedighi, M. & Lea-Langton, A. 2020 Filtration of microplastic spheres by biochar: Removal efficiency and immobilisation mechanisms. *Water Research* **184**, 116165.

Wang, J., Sun, C., Huang, Q.-X., Chi, Y. & Yan, J.-H. 2021 Adsorption and thermal degradation of microplastics from aqueous solutions by Mg/Zn modified magnetic biochars. *Journal of Hazardous Materials* **419**, 126486.

Wu, P., Cai, Z., Jin, H. & Tang, Y. 2019 Adsorption mechanisms of five bisphenol analogues on PVC microplastics. *Science of the Total Environment* **650**, 671–678.

Yang, K., Peng, J., Srinivasakannan, C., Zhang, L., Xia, H. & Duan, X. 2010 Preparation of high surface area activated carbon from coconut shells using microwave heating. *Bioresource Technology* **101** (15), 6163–6169.

Yang, W., Wang, Y., Sharma, P., Li, B., Liu, K., Liu, J., Flury, M. & Shang, J. 2017 Effect of naphthalene on transport and retention of biochar colloids through saturated porous media. *Colloids and Surfaces A – Physicochemical and Engineering Aspects* **530**, 146–154.

Yang, C. H., Wu, W., Zhou, X. T., Hao, Q., Li, T. J. & Liu, Y. Z. 2021 Comparing the sorption of pyrene and its derivatives onto polystyrene microplastics: Insights from experimental and computational studies. *Marine Pollution Bulletin* **173**, 113086.

Yao, S., Ni, N., Li, X. A., Wang, N., Bian, Y. R., Jiang, X., Song, Y., Bolan, N. S., Zhang, Q. Z. & Tsang, D. C. W. 2023 Interactions between white and black carbon in water: A case study of concurrent aging of microplastics and biochar. *Water Research* **238**, 120006.

Ye, S., Cheng, M., Zeng, G., Tan, X., Wu, H., Liang, J., Shen, M., Song, B., Liu, J., Yang, H. & Zhang, Y. 2020 Insights into catalytic removal and separation of attached metals from natural-aged microplastics by magnetic biochar activating oxidation process. *Water Research* **179**, 115876.

Zhang, K. & Sun, H. 2018 Adsorption of organic pollutants on (degradable) microplastics and the influences on their bioavailability. *Environmental Chemistry* **37** (3), 375–382.

Zhang, Q. L., Lin, Y. C., Chen, X. & Gao, N. Y. 2007 A method for preparing ferric activated carbon composites adsorbents to remove arsenic from drinking water. *Journal of Hazardous Materials* **148** (3), 671–678.

Zhang, K., Gong, W., Lv, J., Xiong, X. & Wu, C. 2015 Accumulation of floating microplastics behind the Three Gorges Dam. *Environmental Pollution* **204**, 117–123.

Zhang, X., Lin, X., He, Y., Chen, Y., Zhou, J. & Luo, X. 2018 Adsorption of phosphorus from slaughterhouse wastewater by carboxymethyl konjac glucomannan loaded with lanthanum. *International Journal of Biological Macromolecules* **119**, 105–115.

Zhong, Q., Lin, Q., He, W., Fu, H., Huang, Z., Wang, Y. & Wu, L. 2021 Study on the nonradical pathways of nitrogen-doped biochar activating persulfate for tetracycline degradation. *Separation and Purification Technology* **276**, 119354.

Zhou, X., Liu, Y., Zhou, J., Guo, J., Ren, J. & Zhou, F. 2018 Efficient removal of lead from aqueous solution by urea-functionalized magnetic biochar: Preparation, characterization and mechanism study. *Journal of the Taiwan Institute of Chemical Engineers* **91**, 457–467.

Zhou, Z. Y., Zhang, P. Y., Zhang, G. M., Wang, S. Q., Cai, Y. J. & Wang, H. J. 2021 Vertical microplastic distribution in sediments of Fuhe River Estuary to Baiyangdian Wetland in Northern China. *Chemosphere* **280**, 130800.

First received 21 November 2023; accepted in revised form 24 March 2024. Available online 4 April 2024